Weak Values and Quantum Information in Scattering Physics — New Theoretical and Experimental Effects

C Aris Chatzidimitriou-Dreismann

Institute of Chemistry, Sekr. C2, Faculty II, Technical University of Berlin, D-10623 Berlin, Germany

E-mail: chariton.dreismann@tu-berlin.de

Abstract. Weak Values (WV) and Two-State-Vector Formalism (TSVF) provide novel insights in various quantum physical and technological fields. In the first part of the paper we consider a new quantum effect of scattering accompanying an elementary collision of two quantum systems A and B, in which the latter interacts with a quantum environment. In clear contrast to a classical environment, the quantum case can exhibit counter-intuitive effects of momentum- and energy-transfer which contradict conventional expectations. Experimental evidence of a new effect—deficit of momentum transfer (equivalently: reduced effective mass) in a neutron-atom collision—is presented and theoretically interpreted. Here, non-relativistic incoherent inelastic neutron scattering (INS) is applied. INS on single H_2 molecules confined in multi-walled carbon nanotube channels has been experimentally investigated. Interpreted within conventional theory, the results reveal a counter-intuitive reduced effective mass of the recoiling H_2 molecule, i.e. $M = 0.64$ a.m.u. (atomic mass units). In contrast, this finding has a simple qualitative interpretation within WV and TSVF theory. In the second part of the paper we report on current experimental and theoretical investigations in the field of X-ray diffraction (XRD), which belongs to coherent scattering. Preliminary XRD results from cubic crystalline materials show a surprising variation of the measured lattice parameter (usually called "lattice constant") with momentum transfer. A first theoretical model of the effect in the light of the new theory is presented. These findings give further evidence for the broad character and significance of the novel WV and TSVF theory.

1. Introduction

The fundamental time-inversion symmetry of the Schrödinger equation was shown to be a crucial feature in the novel theory of Weak Values (WV) and the Two-State Vector Formalism (TSVF) of Aharonov and collaborators; cf. [1, 2, 3, 4, 5, 6, 7, 8] and references therein. New experiments were proposed based on this theory, and several novel quantum effects were experimentally confirmed; see e.g. [9, 10, 11] and references therein. In these works also the physical reality of the wavefunction was further exposed and clarified [10].

In this paper, the focus is mainly on the potential applicability of the general WV-TSVF theory to real scattering experiments, rather than on pure theoretical or interpretational issues. The conceptual power of the theory is exemplified with the aid of an experimental result from inelastic incoherent neutron scattering (INS) of H_2 in carbon nanotubes and related nanostructured materials, as obtained with modern 2-*dimensional* neutron spectrometers. It is shown that the measured mass of the roto-translating H_2 molecule moving along the nanotube axis—if interpreted with conventional theory—appears to be $M = 0.64 \pm 0.07$ a.m.u. (atomic mass units)!

In short, our findings correspond to a striking new effect: a strong *effective mass deficit* of the scattering object—or, equivalently, a corresponding *momentum transfer deficit*; see Section 4 for a concise description of recent investigations [15, 16, 17]. No known conventional theoretical interpretation of this finding exists until now [17].

We further report about current investigations concerning a new possible application of the theory in the field of "coherent scattering", in particular X-ray diffraction (XRD) from crystalline solid material. Preliminary experimental findings indicate that the well known single lattice parameter a of a cubic system, (e.g. silicon, Si) is not a constant, but it varies with scattering (or diffraction) angle and thus with applied momentum transfer. A first theoretical WV-TSVF model is given. The main theoretical result reveals the necessary conditions for the new effect to occur and shows two sufficient approximations for the conventional result to hold; see Section 5.

These investigations have been strongly motivated by the work of Aharonov et al. [21], which provided a remarkably simple and clear theoretical model demonstrating the predictive power of the new theory. Here, an "anomalous" momentum exchange between photons (or particles) passing through a Mach-Zehnder interferometer (MZI) and one of its mirrors is predicted. The surprising predicted new effect is, essentially, as follows: Although the photons (particles) collide with the considered mirror only from the inside of the MZI, they do not push the mirror outwards, but rather they somehow succeed to pull it in [21]; see Section 3.

The theory of WV and the TSVF are nowadays active areas of research, providing new conceptual ideas and novel experimental techniques for a wide range of applications. In the present paper, however, interpretational issues play a minor role; instead, the focus is a new family of experiments related to momentum and/or energy transfers, thus contributing to the connection between the "theory"-community and the community of experimental scattering and diffraction physics; cf. in particular [17].

Finally the following remark may be in order. The present paper is based on, and extends, the presentation [16] given at the previous SiS-XVII conference (Bregenz, 2017). Therefore, certain lengthy theoretical derivations concerning weak values in incoherent scattering (like INS) are only cited and not repeated here explicitly.

2. On Weak Values, Two-State-Vector-Formalism and impulsive Weak Measurements

Let us start with the following short remarks about the new theory of WV and TSVF. Consider the well known formula for the expectation value of standard quantum mechanics,

$$\langle A\rangle = \langle\psi_i|\hat{A}|\psi_i\rangle \tag{1}$$

where $\hat{A}$ is the operator (i.e. an observable) whose value is to be measured and $|\psi_i\rangle$ is the initial state of the system (just before the measurement, as prepared by the experimenter). As $\hat{A}$ is Hermitian, $\langle A\rangle$ is a real number.

Now consider the formal expression

$$A^w \equiv \frac{\langle\psi_f|\hat{A}|\psi_i\rangle}{\langle\psi_f|\psi_i\rangle} \tag{2}$$

where $|\psi_f\rangle$ is the final state of the system (i.e., after the measurement interaction). In general, A^w is a complex number. A^w is the weak value of $\hat{A}$ of a system experimentally prepared in the state $|\psi_i\rangle$ and experimentally postselected in the state $|\psi_f\rangle$ [1]. It should be emphasized that both real and imaginary parts of A^w are *experimentally measurable* quantities; see e.g. the review article [11].

One immediately sees that

$$\text{if} \quad |\psi_i\rangle = |\psi_f\rangle \quad \text{then} \quad \langle A\rangle = A^w \tag{3}$$

Thus Eq. (2) represents a generalization of the standard definition Eq. (1).

Furthermore, consider again the conventional expectation value of an observable $\hat{A}$, Eq. (1) and suppose $|\psi_i\rangle = \sum_j c_j|j\rangle$, where the kets $\{|j\rangle\}$ represent an orthogonal basis. Let us assume that we make a measurement of the observable $\hat{A}$ using the above basis and we make a postselection with respect to the final state $|j\rangle$. That is, we make a strong projective measurement corresponding to the projector $|j\rangle\langle j|$. If one is interested in the average (mean value) of the measuring results, one has:

$$\langle\psi_i|\hat{A}|\psi_i\rangle = \sum_j c_j^*\langle j|\hat{A}|\psi_i\rangle = \sum_j |c_j|^2 \frac{\langle j|\hat{A}|\psi_i\rangle}{\langle j|\psi_i\rangle} \equiv \sum_j |c_j|^2 A^w_{j,\psi_i} \tag{4}$$

where A^w_{j,ψ_i} is the WV of $\hat{A}$ with pre-selected state $|\psi_i\rangle$ and post-selected state $|j\rangle$, and $|c_j|^2$ is the probability for the occurance of $|j\rangle$; cf. [5]. These relations show that (possibly existing) specific effects captured by some (measurable!) weak values A^w_{j,ψ_i} may become "smeared out" in the average $\langle\psi_i|\hat{A}|\psi_i\rangle$ of conventional quantum mechanics—if the individual weak values do possess any physical meaning.

Indeed, Aharonov and collaborators have revealed the crucial physical significance of Eq. (2); i.e., in specific and well-defined experimental setups, weak values are new *measurable* quantities [1]! This corresponds to a novelty, or discovery, since weak values are unknown in standard quantum mechanics (cf. e.g. the Feynman Lectures [12]).

The measurement in WV-TSVF theory is described by an impulsive von Neumann process [23], introducing a pointer (or measuring apparatus) with wavefunction $|\Phi\rangle$. It should be emphasized that the pointer is a *quantum* object, too. Let the interaction Hamiltonian be

$$H_{int} = g\delta(t - t_0)\,\hat{A} \otimes \hat{M} \tag{5}$$

where g is a (small and real) coupling constant, $\delta(t - t_0)$ is the delta function, and $\hat{M}$ is the operator of the coupling quantity of the pointer. $\hat{A}$ is the operator of the system's quantity to be measured. The interaction is impulsive and thus one is interested in the time evolution during a short time interval around t_0, which allows to neglect (in the calculations) the "free" evolution before and after t_0.

A standard von Neumann (also called "strong") measurement yields the eigenvalues of the measureds observable, but at the same time disturbs the measured system. This changes the system's initial state and the final state is an eigenstate of the observable's operator. On the other hand, by coupling a measuring device to a system sufficiently weakly, i.e. performing a Weak Measurement (WM), it may be possible to read out certain information while limiting the disturbance induced by the measurement to the system. As Aharonov and collaborators originally proposed [3, 2], new physical insights are revealed when one furthermore post-selects on a particular outcome of the experiment.

Before the interaction occurs, let the initial system-apparatus state be $\psi_i \otimes \Phi_i$. After the interaction, this state evolves as

$$\psi_i \otimes \Phi_i \to e^{-ig\hat{A}\otimes\hat{M}}\psi_i \otimes \Phi_i \tag{6}$$

(temporarily with $\hbar = 1$, for convenience). Now the following point is a crucial element of TSVF: We post-select (with a strong measurement) a final state of the system, ψ_f. We are interested

in the associated apparatus' final state, Φ_f, from which the measuring result can be determined. Φ_f is obtained by tracing out the system's variables:

$$\Phi_f = \langle\psi_f|e^{-ig\hat{A}\otimes\hat{M}}|\psi_i\rangle\Phi_i \tag{7}$$

and for a sufficiently weak interaction (i.e., small g) one obtains through power expansion

$$\Phi_f \approx \langle\psi_f|1 - ig\hat{A}\otimes\hat{M}|\psi_i\rangle\Phi_i = \langle\psi_f|\psi_i\rangle(1 - igA^w\hat{M})\Phi_i \approx \langle\psi_f|\psi_i\rangle e^{-igA^w\hat{M}}\,\Phi_i \tag{8}$$

Here, A^w is the aforementioned WV of the system variable $\hat{A}$; one assumes $\langle\psi_f|\psi_i\rangle \neq 0$. Thus the state of the measuring device evolves with an effective *one-body* Hamiltonian $\hat{H}_M = gA^w\hat{M}$, i.e.,

$$\Phi_i \to e^{-igA^w\hat{M}}\Phi_i\,. \tag{9}$$

Thus we arrive at the interesting result that the pointer dynamics depends on the three dynamical quantities $\hat{A}$, $|\psi_i\rangle$ and $|\psi_f\rangle$ only through the single complex number A^w.

In one part of the following theoretical considerations, in particular those dealing with the recent XRD investigations, we will make the choice

$$\hat{M} = \hat{p}\,, \tag{10}$$

i.e., the pointer variable will be its momentum. We will also need the variance of the initial pointer state

$$Var_p = \langle\Phi_i|\hat{p}^2|\Phi_i\rangle - \langle\Phi_i|\hat{p}|\Phi_i\rangle^2 \tag{11}$$

For the theoretical modeling of the XRD results presented below, the imaginary part $Im[A^w]$ of the weak value A^w is of particular interest. Namely, according to the general WV-TSVF theory, the measured mean pointer momentum after the interaction (i.e., in its final state) changes from its initial value $\langle p\rangle_i$ to its final value

$$\langle p\rangle_f = \langle p\rangle_i + 2\,g\,Im[A^w]\,Var_p\,. \tag{12}$$

Additionally, the real part of the weak value, $Re[A^w]$, is measured by the position (say, x) shift of the pointer, i.e.

$$\langle x\rangle_f = \langle x\rangle_i + g\,Re[A^w]\,. \tag{13}$$

For full derivations, see e.g. [13, 5].

2.1. On the Elitzur-Vaidman effect, quantum computers, and the interpretation of the quantum state vector

One overarching open question concerning the interpretation of quantum physics—the "meaning" of the wavefunction—appears to be in part answered by these recent developments.

The possibility that the wavefunction (or, more general, the state vector) is purely epistemological, i.e. solely a mathematical quantity representing the observer's knowledge, is often associated with the well-known Copenhagen interpretation, sometimes also called the "orthodox" interpretation of quantum mechanics. An ingredient of this is to consider the state vector to be associated with an ensemble of quantum systems, but not with individual ones.

The alternative, and recently emerging, viewpoint is to regard the state vector as an ontological entity, or a "real" physical entity; this is also the viewpoint supported by the novel WV-TSVF theory. An ingredient of this interpretational or theoretical viewpoint is to consider the state vector to be associated with an individual quantum system (at least in specific and well

defined experiments). Clearly, this viewpoint was unacceptable for the majority of physicists in the last century.

In this context, the counter-intuitive Elitzur-Vaidman effect [18] concerning *interaction-free* measurements (IFM, popularly also known as "bomb tester") revealed the ability to experimentally obtain information about an object's presence in some spatial region without ever "touching" it. Certainly, this is a paradox in the frame of classical physics. Namely, in successful interaction-free "bomb detections", absolutely no known physical quantity—e.g. energy, momentum, angular momentum, spin, force, etc.—has been exchanged between the object and the probe particle (e.g. a photon or a neutron). However, this physical information cannot be gained "at no charge". The related "costs" are provided by the photon's (neutron's) wavefunction, following the principles of IFM. Therefore, the experimental verification of this novel quantum effect strongly suggests that the quantum-mechanical wavefunction is a real physical quantity—and not just an auxiliary construct for the calculation of expectation values of quantum observables.

However, the interpretation of the quantum state vector has recently become relevant to practical applications such as quantum cryptography and quantum computation; see e.g. the achievement to demonstrate experimentally the so-called "quantum supremacy", using GOOGLE's programmable quantum processor *Sycamore* with 53 qubits and executing a specific computational task [19]. Remarkably, therein the authors report a (very specific) quantum computational task being performed in about 200 seconds—in contrast to the estimated 10,000 years needed by the (presently existing) most powerful classical supercomputer to perform the same task. To stress this point, in simplified terms: The state vector calculated by the GOOGLE processor is a physical quantity that refers to one *single* quantum processor (i.e., one quantum system), and *not* to an *ensemble* of quantum processors.

In this context it should also be mentioned the very recent (December 2019) quantum optical achievement [20], in which boson sampling—using 20 photons in a 10^{14}-dimensional Hilbert space—is applied towards demonstrating the quantum computational supremacy.

2.2. An additional observation about the meaning of WV and TSVF

Some additional remarks and/or explanations regarding the formal structure of WV-TSVF may be appropriate at this point. The starting point is the von Neumann-type impulsive interaction Hamiltonian, Eq. (5). We consider here an insightful result derived by Pati and Wu [14].

We make use of the formula (see e.g. [1], p. 39, or [14])

$$\hat{A}|\psi_i\rangle = \langle\hat{A}\rangle|\psi_i\rangle + \Delta\hat{A}|\overline{\psi}_i\rangle \tag{14}$$

where $|\overline{\psi}_i\rangle$ is a state orthogonal to $|\psi_i\rangle$, $\langle\hat{A}\rangle = \langle\psi_i|\hat{A}|\psi_i\rangle$, and $\Delta\hat{A}$ is the uncertainty in the state $|\psi_i\rangle$, i.e. $(\Delta\hat{A})^2 = \langle\psi_i|(\hat{A} - \langle\hat{A}\rangle)^2|\psi_i\rangle$. Applying $\langle\psi_f|$ to both sides of Eq. (14) we obtain

$$A^w = \langle\hat{A}\rangle + \Delta\hat{A}\frac{\langle\psi_f|\overline{\psi}_i\rangle}{\langle\psi_f|\psi_i\rangle} \equiv \langle\hat{A}\rangle + \delta A_w \tag{15}$$

This result sheds additional light on a crucial reason for the difference δA_w between the conventional expectation value $\langle\hat{A}\rangle$ and the WV A^w: a non-vanishing uncertainty $\Delta\hat{A} > 0$ accompanied with a non-vanishing scalar product $\langle\psi_f|\overline{\psi}_i\rangle \neq 0$. In particular, the physical meaning of the latter is that the two states $|\psi_f\rangle$ and $|\overline{\psi}_i\rangle$ have the ability to *produce quantum interferences*.

In summary: This short derivation demonstrates that the novel features of WV and TSVF are caused by *quantum interference* between the post-selected state and another quantum state which is orthogonal to the pre-selected state [14]. In other words, this result also stresses the importance of both concepts: the conventional "pre-selected initial state" *and* the "post-selected final state".

3. How Weak Values appear in derivations—A didactical example

Here we consider a surprisingly simple theoretical model by Aharonov et al. [21] mentioned in the Introduction, which also motivated several of our investigations. The presentation is mainly taken from Refs. [16, 17].

A specific result of [21] concerns "anomalous" momentum transfer between two quantum objects (i.e. a photon and a mirror) and thus appears to be in intimate connection with our neutron-atom collision (or scattering) experiments considered below. The schematic representation of the experimental setup is shown in Fig. 1.

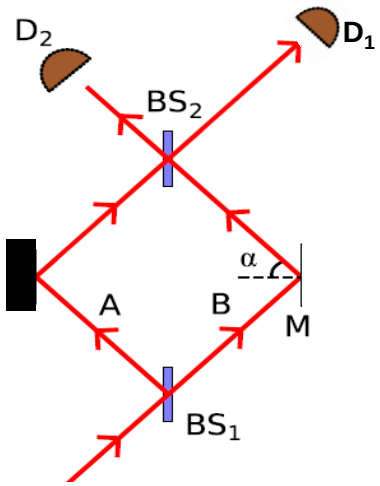

Figure 1. Mach-Zehnder interferometer (MZI) and path of a light beam (or a particle, etc.). The mirror M is a nanoscopic *quantum* object. Of particular interest are the photons (particles) emerging toward detector D_2. (Taken from [16] with permission.)

A photon (or particle) beam enters a device similar to a usual Mach-Zehnder interferometer (MZI), with the exception that one reflecting mirror is sufficiently small (say, a meso- or nanoscopic object M) in order that its momentum distribution may be detectable by a suitable non-demolition measurement [22]. In Ref. [21] the following astonishing result was derived. Although the post-selected photons (as all photons do, of course) collide with the mirror M only from the *inside* of the MZI, they do not push M outwards, but rather they somehow succeed to *pull it in*. It is obvious that this result cannot have any conventional theoretical interpretation.

Let us now shortly outline the theoretical derivation of this effect, following the presentation of Ref. [21] closely. The two beam splitters have both the same non-equal reflectivity r and transmissivity t (both real, with $r^2 + t^2 = 1$). Here we assume $r > t$. Thus, when a single photon (particle) enters the MZI by impinging on the left side of the beam splitter BS_1, the probabilities to be found in the arms A and B are r^2 and t^2, respectively.

Using the standard convention, an incoming state $|\text{in}\rangle$ impinging on the beam splitter will emerge as a superposition of a reflected state $|R\rangle$ and a transmitted state $|T\rangle$; $|\text{in}\rangle \rightarrow ir|R\rangle + t|T\rangle$. Hence when a single photon impinges from the left on BS_1, as illustrated in Fig. 1, the effect of the beam splitter is to produce inside the interferometer the state

$$|\Psi\rangle = ir|A\rangle + t|B\rangle \tag{16}$$

where $|A\rangle$ and $|B\rangle$ denote the photon propagating along the A and B arms of the interferometer, respectively.

As assumed above, the second beam splitter BS_2 is identical to the first. Thus one can readily check that a photon in the quantum state $|\Phi_1\rangle = t|A\rangle - ir|B\rangle$ impinging on the second beam splitter, emerges towards detector D_1, while a photon in the orthogonal state $|\Phi_2\rangle = -ir|A\rangle + t|B\rangle$ emerges towards detector D_2.

If we send a *classical* photon beam towards this interferometer, then it is obvious that this pushes the mirror M outward. Let us now send a *quantum* beam of photons (or particles) into the MZI. Each photon incident on M gives it a momentum kick δ. Note that each individual momentum kick must be much smaller than the spread Δ of momentum of the mirror M. This is a general property of any interferometer. It has to be so in order to maintain the coherence of the beam in the interferometer. Accordingly, if $\phi(p)$ is the initial quantum state of M and $|\Psi\rangle$ the quantum state of the photon after the input beam splitter BS_1, but before reaching M, the reflection on the mirror M results in

$$|\Psi\rangle\phi(p) = (ir|A\rangle + t|B\rangle)\phi(p) \to ir|A\rangle\phi(p) + t|B\rangle\phi(p-\delta) \tag{17}$$

(This holds before the photon reaches the second beam splitter BS_2.)

If $\phi(p)$ is orthogonal to $\phi(p-\delta)$ where δ is the kick given by the photon, then the photon ends up entangled with the mirror and coherence is lost. Another way of looking at this is to note that the mirror has to be localized within a distance smaller than the wavelength of light, otherwise there will be phase fluctuations larger than 2π and interference is lost.

For simplicity we take the state of the mirror to be (up to normalisation) $\phi(p) = \exp(-\frac{p^2}{2\Delta^2})$. Consider now a single photon propagating through the interferometer. Given that $\delta \ll \Delta$, we can approximate the state (17) of the photon and mirror just before the photon reaches the output beam splitter by

$$|\Psi\rangle\phi(p) \approx ir|A\rangle\phi(p) + t|B\rangle\Big(\phi(p) - \frac{d\phi(p)}{dp}\delta\Big) = |\Psi\rangle\phi(p) - t|B\rangle\frac{d\phi(p)}{dp}\delta \tag{18}$$

We now consider the following particular case, which may appear to be "innocent" or "without any particular physical interest": We analyze the effect caused by photons emerging in the beam directed towards D_2 only. (Clearly, modern single-photon counting setups can do it.)

The state of the mirror M is then given (up to normalization) by projecting the joint state onto the state of the photon corresponding to this beam, i.e.

$$\begin{aligned}
\langle\Phi_2|\Big(|\Psi\rangle\phi(p) - t|B\rangle\frac{d\phi(p)}{dp}\delta\Big) &= \langle\Phi_2|\Psi\rangle\Big(\phi(p) - \frac{t\langle\Phi_2|B\rangle}{\langle\Phi_2|\Psi\rangle}\frac{d\phi(p)}{dp}\delta\Big) \\
&= \langle\Phi_2|\Psi\rangle\Big(\phi(p) - \frac{\langle\Phi_2|\mathbf{P}_B|\Psi\rangle}{\langle\Phi_2|\Psi\rangle}\frac{d\phi(p)}{dp}\delta\Big) \\
&= \langle\Phi_2|\Psi\rangle\phi(p - P_B^w\delta)
\end{aligned} \tag{19}$$

Here $\mathbf{P}_B = |B\rangle\langle B|$ is the *projection operator* on state $|B\rangle$ and

$$P_B^w = \frac{\langle\Phi_2|\mathbf{P}_B|\Psi\rangle}{\langle\Phi_2|\Psi\rangle}$$

is the so called *weak value* (WV) of $\mathbf{P}_B$ between the initial state $|\Psi\rangle$ and the final state $|\Phi_2\rangle$ [1, 3, 4, 5, 6, 11].

The numerical value of P_B^w is calculated straightforward:

$$\begin{aligned} P_B^w &= \frac{\langle\Phi_2|\mathbf{P}_B|\Psi\rangle}{\langle\Phi_2|\Psi\rangle} = \frac{(ir\langle A| + t\langle B|)\mathbf{P}_B(ir|A\rangle + t|B\rangle)}{(ir\langle A| + t\langle B|)(ir|A\rangle + t|B\rangle)} \\ &= -\frac{t^2}{r^2 - t^2} \end{aligned} \tag{20}$$

Hence the momentum kick received by the mirror due to a photon emerging towards D_2 is

$$\delta p_M = P_B^w\,\delta = -\frac{t^2}{r^2 - t^2}\,\delta \tag{21}$$

Since we assumed $r > t$, the sign of the momentum received by the mirror is negative, hence *the mirror is pushed towards the inside* of the MZI. This momentum change is a result of the mirror receiving a *s*uperposition between a kick δ and no kick at all, corresponding to the photon (particle) propagating through the two MZI-arms.

The appearance in the above expressions of the WV of the projector $\mathbf{P}_B$ is not accidental. Indeed, we can view the mirror as a measuring device measuring whether or not the photon is in arm B or not. The momentum of the mirror acts as a "pointer" (no kick — the photon is in arm A; kick — the photon is in arm B). However, since the photon can only change the position of the pointer (i.e. the momentum of the mirror) by far less than its spread, we are in the so called "weak measurement" regime.

Summarizing, the photons that exit the MZI and end up in detector D_2 give *negative* momentum kicks on M, although they collide with the mirror only from the inside of the MZI. Hence, these photons do not push the mirror outwards, but rather they somehow succeed to pull it in. This is a purely quantum effect, being realized by a quantum superposition of giving the mirror zero momentum and positive momentum—the superposition results in the mirror gaining negative momentum [21].

4. Incoherent scattering in view of WV and TSVF

In this section the main theoretical and experimental investigations presented in the previous SiS-XVII conference (Bregenz, 2017) and recently published in [16] are outlined.

4.1. Neutron-atom collision, model Hamiltonian

Now we outline the basic result of WV and TSVF applied to non-relativistic scattering processes, particularly in the physical context of *non-relativistic* neutron scattering, firstly proposed and explored in [15]; see also [17].

The position and momentum of the probe particle (neutron; this corresponds to the pointer) are denoted as (q, p). Similarly, the position and momentum of the scattering system (atom, nucleus) are denoted as (Q, P). $\hat{X}$ represents the operator of the corresponding observable X.

In the following it is sufficient to consider an effective *one-dimensional* problem along the direction of the collisional momentum transfer $\mathbf{K}$, as given by conventional theory. The operator of atomic (nucleus) momentum component parallel to $\mathbf{K}$ is denoted with $\hat{P}$.

Due to momentum conservation in the two-body collision, one expects (n: neutron, or pointer; A: atom, or system)

$$-\hbar K_n = +\hbar K_A \equiv \hbar K > 0, \tag{22}$$

where $+\hbar K_A$ is the momentum transfer *on the atom* due to the collision, and $-\hbar K_n$ is the associated momentum transfer on the neutron. We choose K_A to be positive, following standard notation (e.g. as in [24, 25]).

In [16] we presented in detail the heuristic derivation of a von Neumann-type interaction Hamiltonian which captures momentum and energy transfers. This is based on the energy conservation by the collision of a neutron with an atom: energy-loss of the neutron, is equal to the energy gain of the scattering system. The validity of this energy conservation is best demonstrated with a well known experimental INS-result: scattering from liquid He; see Fig. 2. The red line represents the free recoil parabola

$$E = \frac{(\hbar K)^2}{2M} \tag{23}$$

(M: mass of ^{4}He atom) of the He atom in the $K - E$ plane (often called momentum-energy plane), which fits the measured data excellently. This parabola represents the well-known Impulse Approximation [24, 25]. The original measurements [28] were carried out with the new spectrometer ARCS [27].

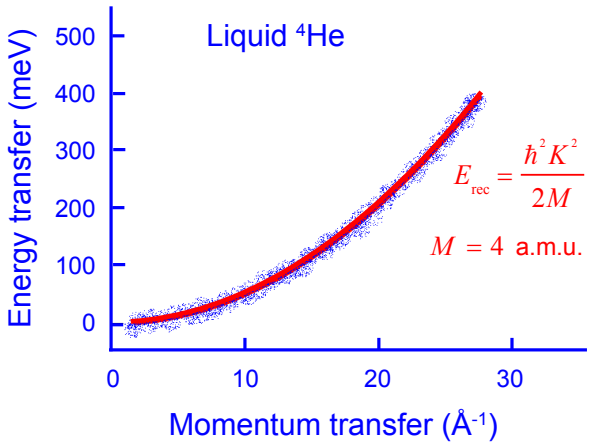

Figure 2. Schematic representation (blue points) of measured dynamic structure factor $S(K, E)$ of liquid helium [28]. The red line is the calculated recoil parabola, according to Eq. (23), for the mass of ^{4}He. The white-blue ribbon around the recoil parabola represent data points measured with the time-of-flight (TOF) spectrometer ARCS [27]. (Taken from Ref. [17] with permission.)

In view of the theory of WV and TSVF, there may exist "small" measurable deviations from the conventionally expected momentum K and energy E transfers. As discussed in [17], these deviations can be formally captured by replacing the atomic momentum $\hat{P}$ with a *small* momentum difference $\hat{P} - \hbar K \hat{I}_A$ ($\hat{I}_A$: identity operator in the atomic subspace). Summarizing, the proposed von Neumann-type model interaction Hamiltonian (describing the deviation from conventional theory) is [15, 16]

$$\Delta \hat{H}_{int}(t) = +g\, \delta(t)\, \hat{q} \otimes (\hat{P} - \hbar K\, \hat{I}_A) \tag{24}$$

($\delta(t)$: delta function; g: smallness parameter). This model Hamiltonian has the usual (von Neumann-type) form (5) of an interaction Hamiltonian [15, 16, 17].

The physical motivation of the two parts of the model Hamiltonian (24) is in line with an associated example by Aharonov et al., which reads as follows: "Consider, for example, an ensemble of electrons hitting a nucleus in a particle collider. [...] The main interaction is purely electromagnetic, but there is also a relativistic and spin-orbit correction in higher orders which can be manifested now in the form of a weak interaction." ([29], p. 3.)

The presence of the "conventional" term $-\hbar K\,\hat{I}_A$ in Eq. (24) causes a slight extension of the general theoretical results Eqs. (12) and (13) for the total numerical values of the measured quantities, e.g.

$$[\langle\hat{p}\rangle_f - \langle\hat{p}\rangle_i]_{\rm total} = [\langle\hat{p}\rangle_f - \langle\hat{p}\rangle_i]_{\rm conventional} + [\langle\hat{p}\rangle_f - \langle\hat{p}\rangle_i]_{\rm correction} \tag{25}$$

cf. [17].

4.2. INS from single H_2 molecules in carbon nanotubes

Another surprising result from incoherent inelastic neutron scattering was observed by Olsen et al. [30] in the quantum excitation spectrum of H_2 adsorbed in multi-walled nanoporous carbon (with pore diameter about 8–20 Å).

The incoherent inelastic neutron scattering (INS, or IINS) experiments were carried out at the new generation TOF spectrometer ARCS of Spallation Neutron Source SNS (Oak Ridge Nat. Lab., USA) [27]. This is a 2-*dimensional* spectrometer, i.e. its detectors (about 100,000) measure a broader area of the $K-E$ plane. The temperature was $T = 23$ K, and the incident neutron energy E_i was 90 meV. The latter implies that the energy transfer cannot excite molecular vibrations (and thus cannot break the molecular bond), but only excite rotation and translation (also called recoil) of H_2 which interacts only weakly with the substrate:

$$E = E_{rot} + E_{trans} \tag{26}$$

The experimental two-dimensional INS intensity map $S(K, E)$ (after background subtraction) is shown in Fig. 3, which is taken from the original paper [30]. The following features are clearly visible. First, the intensive peak centered at $E_{rot} \approx 14.7$ meV is due to the well known first rotational excitation $J = 0 \to 1$ of the H_2 molecule [31]. The wave vector transfer of this peak is $K_{rot} \approx 2.7$ Å^{-1}. Thus the peak position in the K–E plane shows that the experimentally determined mass of H that fulfills the relation $E_{rot} = (\hbar K_{rot})^2/2M_H$ is (within experimental error) the mass M_H of the free H atom,

$$\text{rotation:} \quad M_H = 1.0079 \ \text{ a.m.u.} \tag{27}$$

namely, $M_{eff}(H) = M_H$. (a.m.u.: atomic mass units.) In other words, the location of this rotational excitation in the K–E plane agrees with conventional theoretical expectations for INS, according to which each neutron scatters from a single H [31]. Recall that an agreement with conventional theory was also observed in the case of scattering from ^{4}He [28]; see Fig. 2.

Moreover, the authors provide a detailed analysis of the roto-recoil data from incoherent inelastic neutron scattering, as shown in Fig. 3, and extract a strongly reduced effective mass of the whole recoiling H_2 molecule (left parabola, green line); see Eq. (23):

$$\text{translation (recoil):} \quad M_{eff}(\mathrm{H_2}) \approx 0.64 \pm 0.07 \ \text{ a.m.u.} \tag{28}$$

This is in blatant contrast to the conventionally expected value $M(\mathrm{H_2}) = 2.01$ a.m.u. for a freely recoiling H_2 molecule (right parabola, red line). (Recall that the neutron-molecule collision does not break the molecular bond.) An extensive numerical analysis of the data is presented in [30], being based on conventional theory [24, 31].

This strong reduction of effective mass, which is far beyond any conceivable experimental error. Namely, the observed momentum transfer deficit is about -43% of the conventionally expected momentum transfer. This provides experimental evidence of the new anomalous effect of momentum-transfer deficit under consideration.

As explained in detail in [16], every H_2-substrate conventional binding must increase the molecule's effective mass. Thus these findings from INS are in clear contrast to every

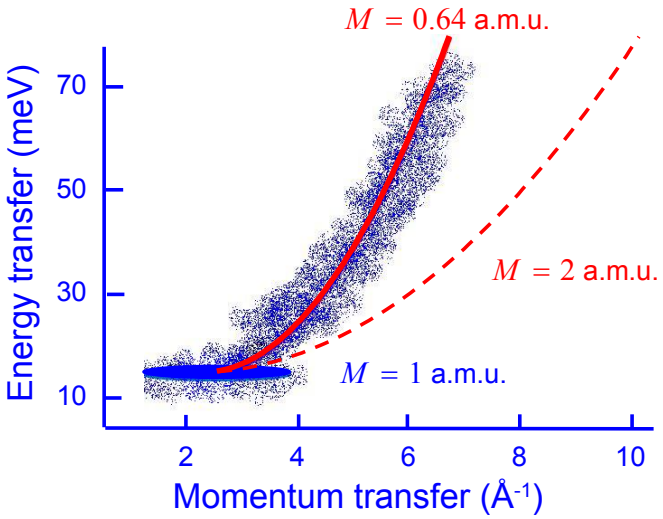

Figure 3. Experimental INS results from H_2 in carbon nanotubes, with incident neutron energy $E_i = 90$ meV; adapted from Figure 1 of Ref. [30]. The translation motion of the recoiling H_2 molecules causes the observed continuum of intensity, usually called "roto-recoil" (white-blue ribbon), starting at the well visible first rotational excitation of H_2 being centered at $E_{rot} \approx 14.7$ meV and $K_{rot} \approx 2.7$ Å^{-1} (blue ellipsoid). The K-E position of the latter is in agreement with conventional theory. In contrast, a detailed fit (red parabola; full line) to the roto-recoil data reveals a strong reduction of the effective mass of recoiling H_2, which appears to be only 0.64 a.m.u. The red dashed line represents the conventional-theoretical parabola with effective mass 2.0 a.m.u. For full details of data analysis, see [30]. (Reproduced from Ref. [15] with permission.)

conventional (classical or quantum) theoretical expectation. However, they have a natural (albeit qualitative, at present) interpretation in the frame of modern theory of WV and TSVF.

The above experimental results also show that the two-dimensional spectroscopic technique, as offered by the advanced TOF-spectrometer ARCS, represents a powerful method that provides novel insights into quantum dynamics of molecules and condensed matter. Clearly, this is due to the fact that K and E transfers can be measured over a broad region of the K–E plane. This advantage makes these new instruments superior to the common *one-dimensional* ones (like TOSCA at ISIS spallation source, UK), in which the detectors can only measure along a single specific trajectory in the K–E plane. (In fact, TOSCA can measure along two such trajectories [33], but this does not affect the present considerations.)

As an example, consider the results of [32] from molecular H_2 adsorbed in single-wall carbon nanotubes (which is similar to the material of [30]) at $T \approx 20$ K, as investigated with TOSCA. Also this paper reports the measurement of the roto-recoil spectrum, but as a function of E only (due to the aforementioned single trajectory in the K–E plane being instrumentally accessible). Therefore for the theoretical analysis of the data the mass of H_2 was *fixed* to its conventionally expected value of 2 a.m.u., and thus the strong anomalous effect, Eq. (28), remained unnoticed; see [32], p. 903.

5. Coherent scattering—Preliminary XRD investigations motivated by WV and TSVF

In view of the theory under consideration, one may regard XRD (and, more generally, coherent scattering) to be related with a quantum interference feature of all possible Feynman paths of

a photon diffracted by the atoms in the crystal layers. It may be emphasized that the X-ray beam is incoherent—although in the usual textbook treatments of Bragg's Law this beam is tacitly treated as being coherent. Thus one should realize that different X-ray photons scattered by the crystal do not interfere and thus do not contribute to the measured diffractogram. To undergraduate students, this appears to be irritating. But, as already Dirac stressed in his textbook: "...Each photon then interferes only with itself. Interference between two different photons never occurs."; see [34], p. 9.

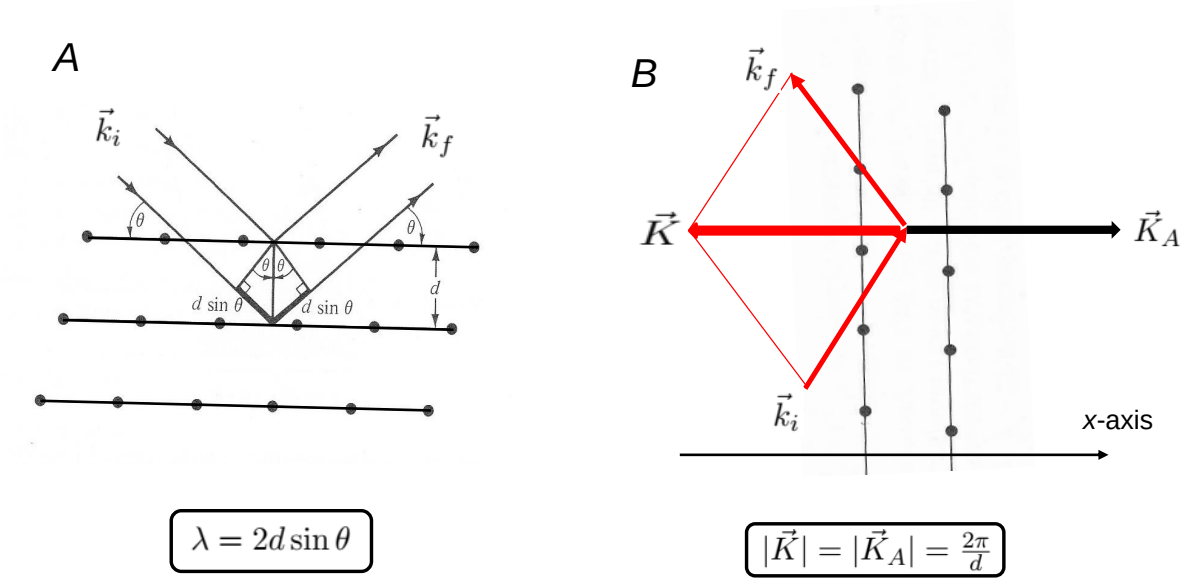

Figure 4. Graphics illustrating Bragg's Law, $\lambda = 2d\sin\theta$ (panel A), and equivalently in momentum space $|\vec{K}| = \frac{2\pi}{d}$ (panel B); see any introductory textbook on solid state physics. $\hbar\vec{K}_A$: momentum transferred to the crystal (system). $\hbar\vec{K}$: momentum transferred to the X-ray photon (pointer, probe). Here, the relations $\vec{K} = \vec{k}_f - \vec{k}_i$ and $\vec{K}_A = -\vec{K}$ hold.

Furthermore, the quantum effect of Aharonov et al. [21] appears in a MZI; see Fig. 1. Intuitively, and with a certain abstraction, one may easily recognize here a "three-layers structure": the two mirrors define two layers and the two beam splitters (which lie on a straight line) constitute the third layer. A photon is "scattered" by this structure, and then is selected in the direction determined by detector D_2 (or D_1).

5.1. XRD: a theoretical model in the light of WV and TSVF

Let us make a heuristic derivation of an interaction Hamiltonian analogous to Eq. (5) or Eq. (24).

The Bragg Law $\lambda = 2d\sin\theta$ (cf. Fig. 4) contains two main factors: the spatial distance between two crystal layers d refers to the system (here a piece of crystal) and the nonlinear term $sin\theta$ refers to the measuring device or "pointer" (see Section 2). However, the equivalent form of the Bragg Law, $K = 2\pi/d$, shows that also the momentum transfer $\hbar K$ (or simply K) describes the pointer. We now may consider a model consisting of two crystal layers (the quantum system A) and the X-photon (the pointer M) being deflected by this system; see Fig. (4). For simplicity of notations, we take the direction of momentum transfer on the system (i.e. K_A), due to scattering of one photon, to be parallel to the x-axis of the laboratory system.

Thus we may consider the following von Neumann-type *ansatz* for the interaction Hamiltonian

$$H_{XRD} = g\,\hat{p}_{photon} \otimes \hat{x}_{crystal} \tag{29}$$

(g: small coupling constant) with the understanding that it should describe a (possibly existing) deviation from the conventional momentum transfer on the deflected photon. By definition, for the conventional expectation value of $\hat{x}_{crystal}$ it should hold $\langle \hat{x}_{crystal} \rangle = d$, for a specific pointer's angular position fulfilling the Bragg condition. This model Hamiltonian contains a momentum and a space variable, so that its physical dimension is that of action, which implies that the small coupling constant g is just a real number (the sign of which is not specified yet).

Now one has to calculate the WV of the system variable $\hat{x}_{crystal} \equiv \hat{X}$, according to Eq. (2)

$$X^w \equiv \frac{\langle \psi_f | \hat{X} | \psi_i \rangle}{\langle \psi_f | \psi_i \rangle} \tag{30}$$

Clearly, the explicit forms of the state vectors in configuration space are very complicated (and time dependent even over a short time interval around t_0). So we may try to perform the calculation in the momentum space—as done in our earlier works [15, 16]. To do so, one has the replacement

$$\hat{X} \to -\frac{\hbar}{i}\frac{\partial}{\partial \hat{P}} \tag{31}$$

where $\hat{P}$ is the associated momentum variable of the quantum system. (Note that the fundamental commutation relation $[\hat{P}, \hat{X}] = \hbar/i$ is fulfilled.)

Let us now calculate X^w in the momentum representation, making the usual assumption of the wavefunctions of initial and final states to be approximated by Gaussians of the same shape (i.e of the form $G(P) = \exp(-P^2/2\sigma_P^2)$). This gives for the nominator

$$\begin{aligned} \langle \psi_f | \hat{X} | \psi_i \rangle &= (-\hbar/i)\langle \psi_f | \frac{\partial}{\partial \hat{P}} | \psi_i \rangle = (-\hbar/i)\langle G(P - \hbar K_A) | \frac{\partial}{\partial \hat{P}} | G(P) \rangle \\ &= (-\hbar/i)(-1/\sigma_P^2)\langle G(P - \hbar K_A) | \hat{P} | G(P) \rangle \\ &= -i\,\hbar/\sigma_P^2\, \langle \psi_f | \hat{P} | \psi_i \rangle \end{aligned} \tag{32}$$

The integral $\langle \psi_f | \hat{P} | \psi_i \rangle$ is exactly the same as that that appeared in the calculation of the WV of momentum P in the treatment of INS; see Section 4 and [15, 16, 17]. Those calculations showed that P^w is real and positive. The same holds true for the denominator of X^w, and thus we immediately arrive at the interesting result that X^w is purely imaginary.

It is in order to repeat here the calculation of P^w, see [16], Eqs. (27,28), (putting in some equations $\hbar = 1$ for brevity):

$$\begin{aligned} P_w &= \frac{\langle G_f | \hat{P} | G_i \rangle}{\langle G_f | G_i \rangle} = \frac{\int dP\, G(P - \hbar K_A)_f P G(P)_i}{\int dP\, G(P - \hbar K_A)_f G(P)_i} \\ &= +\frac{\hbar K_A}{2} = +\frac{\hbar |K|}{2} \end{aligned} \tag{33}$$

The value of the integral in the numerator follows immediately from the following facts: (a) the two functions G are positioned symmetrically around the middle point $\bar{P} = \hbar K_A/2$—one function is centered at 0, the other at $\hbar K_A$; and (b) in this integral P is a linear factor. Note also that this result is independent of the width of the Gaussian G.

Thus we obtain from Eq. (33)

$$X^w = -i\,g\,\hbar/\sigma_P^2 \frac{\hbar |K|}{2} \tag{34}$$

which is a negative imaginary number, (if the smallness parameter g is positive). Parenthetically it may be noted that an imaginary WV is associated with the *back-action* of one system on the second, due to the interaction.

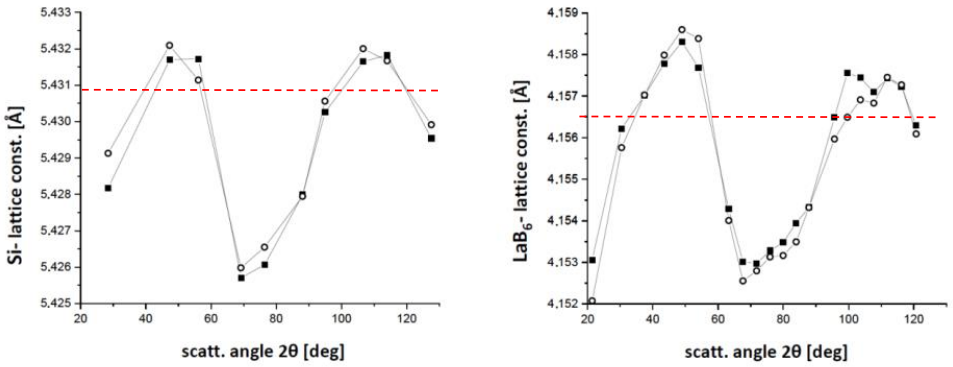

Figure 5. Preliminary results: Measured lattice parameters of Si and LaB_6 (powders; both cubic), determined individually from the scattering angle 2θ of every Bragg peak appearing in the XRD spectrum. That is, the results shown in the Figures contain no fitting parameter. Results of two independent experiments for each material are shown. The typical statistical error of the determined values of the lattice parameter is given by the small difference between the two sets of results in each Figure. The smallness of these differences also demonstrate the long-time reproducibility and/or stability of the XRD instrument. Red dashed lines: Numerical values of lattice constants taken from [35]. (Taken from Ref. [17] with permission.)

We consider now the main result (12) of the WV-TSVF theory [13, 5], which contained the convention $\hbar = 1$. Re-introducing the missing $\hbar$ results in the replacement $A^w \to A^w/\hbar$, as easily seen in the form of the time evolution Eq. (6). Thus we obtain for the WV-correction to the measured pointer momentum

$$\langle p\rangle_f - \langle p\rangle_i = -2\,g/\sigma_P^2 \frac{\hbar|K|}{2}\,Var_p = -g\,\hbar|K|\frac{Var_p}{Var_P} \tag{35}$$

with $Var_P = \sigma_P^2$. We make the following two interesting observations:

(I) This concise theoretical result predicts that the correction term due to the WV-TSVF theory vanishes for the limiting (and idealized) case of a *perfect plane wave* X-ray beam, since then $Var_p = 0$. This is very satisfactory, because it simply reproduces correctly the conventional textbook results of XRD.

(II) Moreover, if the crystal layers would be objects having sharp-valued positions, then, due to the uncertainty relations, the variance of their momenta would become infinite, i.e. $1/Var_P \to 0$ and thus the correction term (35) vanishes. Hence, also this limit reproduces the the conventional textbook results of XRD.

Furthermore, since the conventional change of the pointer's value $(\vec{p}_f - \vec{p}_i)$ is equal to $-K$ along the x-axis (by definition; see Fig. 4), we obtain

$$\begin{aligned}[\langle\hat{p}\rangle_f - \langle\hat{p}\rangle_i]_{\text{total}} &= [\langle\hat{p}\rangle_f - \langle\hat{p}\rangle_i]_{\text{conventional}} + [\langle\hat{p}\rangle_f - \langle\hat{p}\rangle_i]_{\text{correction}} \\ &= -K - g\,\hbar|K|\frac{Var_p}{Var_P}\end{aligned} \tag{36}$$

cf. Eq. (25) and [17]. Moreover, from the preliminary results presented below, we see that the larger deviation from the conventionally expected d appears at about $2\theta \approx 60^\circ - 85^\circ$ and is negative. This conventionally corresponds to an "anomalous increase" of momentum transfer on the photon, since $|K| = 2\pi/d$. This furthermore implies the following nontrivial result:

(III) At least for the three materials under investigation, the coupling constant g in the model Hamiltonian (29) must be positive, $g > 0$. This seems to be a new feature of the general theory of light-matter interaction, being revealed by WV-TSVF theory.

Summarizing, the limiting cases (I) and (II), which reproduce conventional XRD theory, may shed further light on the novel character of WV-TSVF theory.

5.2. Preliminary XRD experiments

These considerations lead to the speculative idea of possible similar "anomalies" that might be measurable in some well known multilayered structures: crystalline solids like e.g. silicon (Si).

The 100-years old XRD (X-ray diffraction) method, and the well known Bragg diffraction law, provide a means to test this intuitive idea. Recently we initiated XRD investigations on some inorganic crystalline materials, e.g. on Si and LaB_6, both being cubic systems, which highly facilitates the analysis of the measured XRD data. (LaB_6 is the standard material used for calibration and other checks of most XRD spectrometers.) Figure 5 shows results of one experimental series about one year ago, using a transmission XRD spectrometer (system STADI P of STOE-GmbH, Darmstadt).

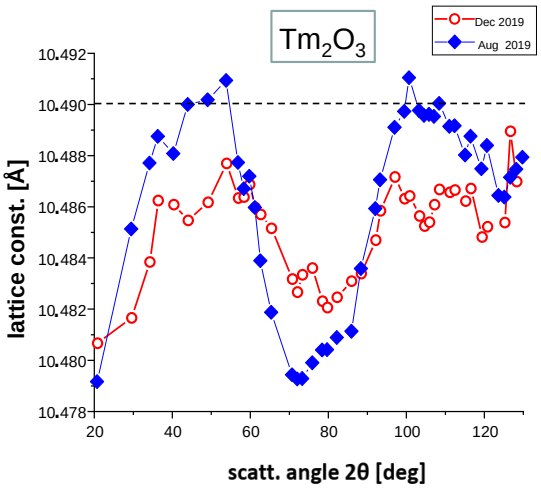

Figure 6. Currently measured lattice parameter of the cubic system Tm_2O_3 (a rare earth oxide); preliminary results. Horizontal broken line: Numerical value of lattice constant taken from the literature. Blue full squares: measurement with optimal alignment of the XRD instrument. Open red circles: measurement with intended misalignment of the XRD instrument, aiming for changing the beam's coherence properties at the scattering spot.

The preliminary findings show that the observed "oscillating" variation of the lattice parameter (the so-called lattice constant) of both materials is well reproducible; see Fig. 5. These results are free of fitting parameters (which is only possible for cubic crystals). In view of the WV-TSVF theory, this striking finding may be understood as follows: There is an unknown momentum-transfer variation in the coherent "multi-layer scattering process" (i.e., in X-ray diffraction) that depends on the scattering angle 2θ (or on the interlayer distance d, as well on the corresponding momentum transfer $\hbar K$) of each measured individual diffraction peak.

Fig. 6 shows first XRD results (using the same diffractometer) from the cubic rare earth oxide Tm_2O_3, which has a larger lattic parameter and thus a larger number of diffraction peaks. Here we also investigated a (theoretically expected) possible change of the new effect with respect to the coherence properties of the X-ray beam. For this, we made a misalignment of the diffractometer, i.e. we made the calibration intentionally worse than possible. This led to a ca. 50% reduction of the "oscillation" observed in the results. Hence this finding supports the physical insight obtained with the aid of the theoretical result Eq. (35).

Clearly, the present simple theoretical model does not capture the full "oscillatory" form shown in Figs. 5 and 6.

Further experiments with different materials and XRD instruments are in preparation.

6. Discussion

The novel theory of WV and TSVF reveals several counter-intuitive effects which may appear "strange" or even "wrong". In order to facilitate their understanding, here we provide additional remarks and explanations.

(*a*) In our theoretical model on neutron scattering (INS), the two operators $\hat{q}$ and $\hat{P}$ occurring in the von Neumann-type interaction Hamiltonian of Eq. (24) refer to two *different* quantum systems. Hence, as Vaidman [36] pointed out, the concept of WV arises here due to the interference of a quantum *entangled* wave and therefore it has no analog in classical wave interference. This further supports the conclusion that WV is a genuinely quantum concept and not some kind of "approximation". In contrast, conventional neutron scattering theory [24, 25, 26] usually treats the neutron as a classical plane wave. To see this, consider the basic formulas of the theory, e.g. the expression for the partial differential cross-section

$$\frac{d^2\sigma_A}{d\Omega d\omega} = const. \cdot \frac{k_f}{k_i} b_A^2 S(\mathbf{K}, \omega) \tag{37}$$

($E = \hbar\omega$, $d\Omega$: solid angle measured/covered by the detector.) $S(\mathbf{K}, \omega)$ is the dynamic structure factor of the scattering system, which contains degrees-of-freedom of the scatterer only. This equation contains *no dynamical* variable of the neutron at all—the neutron is "downgraded" to a classical object and only the scattering length b_A, a *c*-number, appears here. This is a specific feature of the first Born approximation and first-order perturbation theory which the conventional theory is based on [24, 25, 26].

(*b*) The momentum transfer deficit, and the associated effective-mass reduction of the scattering particle A, may appear to someone as violating the energy and momentum conservation laws of basic physics. However, this is not the case, because the scatterer A is *not* an isolated, but an *open* quantum system. Thus we may say that the quantum dynamics of the "environment" of A, which participates to the neutron-A scattering, is indispensable for the new WV-TSVF effect under consideration. Thus it may be helpful to write down the "conservation" relations

$$E_{H+env} = -E_n \quad \text{and} \quad \hbar K_{H+env} = -\hbar K_n \tag{38}$$

which express energy and momentum conservation for the case that the *environment* (indicated with the subscript *"env"*) of the scattering H is not neglected.

(*c*) The INS results from H_2 in C-nanotubes [30] discussed above may appear contradictory—in the frame of conventional theory—because: (*i*) The observed $J = 0 \to 1$ rotational excitation of the H_2 molecule exhibits a $M_{eff} \approx 1$ a.m.u., as conventionally expected. Namely, since the scattering is incoherent, the neutron exchanges energy and momentum with one H-atom only. (*ii*) In contrast, the M_{eff} of the observed translational roto-recoil response of the whole H_2 molecule is not 2 a.m.u. (as expected by conventional theory because the whole H_2 undergoes

a translational motion), but only $M_{eff} \approx 0.64$ a.m.u., see Eq. (28). However, this "conflict" just disappears in the light of the new theory, because it simply implies that the quantum *environment* of H in case (*i*) must be *different* from that in case (*ii*)—the locally rotating H_2 is much less influenced by its environmental interactions than the translating H_2, which necessarily interacts with a greater part of the nanotube during its translational motion due to the collision. In more theoretical words: Different environments effectuate different postselections of the H_2 final state.

(*d*) It is widely believed that INS is not subject to any selection rules; see e.g. the INS textbook [31]. However, an unexpected selection rule was recently discovered for the rotation-translation dynamics of a single H_2 molecule in a C_{60} fullerene ($H_2@C_{60}$), resulting in forbidden INS roto-translational transitions; see Refs. [37, 38] and papers cited therein. In the light of the WV-TSVF results concerning H_2 in C-nanotubes, see Section 4.2, we may predict some related (and experimentally measurable) "anomalous" momentum transfer deficit in $H_2@C_{60}$ too.

(*e*) In Ref. [35] are reported high precision XRD measurements of Si and LaB_6 standard reference materials (i.e., well characterized samples), and especially the relation of their lattice parameters. The authors report a serious discrepancy of *nine* standard deviations from the conventional expectations, which furthermore was shown to remain consistent over a broad range of X-ray energy (5-20 keV). Presently it is not known whether these results are related with the WV-TSVF effect presented in Section 5.

(*f*) In theoretical papers one often meets the criticism that *postselection* just means "throwing out some data"; cf. [39]. In the experimental context at issue, however, post-selection certainly means "performing a concrete measurement on the system, using a well defined detector, and analyzing the measured data only". However, the many applications and new predicted effects of this theory clearly demonstrate that "postselection" is a genuine physical concept, as e.g. pointed out in Ref. [40]

(*g*) Quantum interference and entanglement [41] effects have been recognized to be crucial for quantum computing and quantum information theory; cf. [42] and the very recent Refs. [19, 20]. Hence it would be interesting to explore a potential applicability of the new quantum features offered by WV-TSVF to recently emerging fields of quantum computational complexity theory [43, 44] and ICT (information and communication technology). Namely, WV and TSVF appear to further make available *a new kind of quantum information*—like e.g., the correlation between momentum transferred on the mirror M and the photon measured with detector D_2 in the example of Section 3—the existence of which was unknown thus far. However, here it must be emphasized that the so-called "quantum supremacy" [19] of quantum computation for a fundamental problem, e.g. an NP-complete one, has not been theoretically proven until now [43, 44, 45].

(*h*) In view of the experimentally detected effective-mass reduction, Section 4, it seems appropriate to mention here some speculative ideas concerning a possible technological importance of the new theory. Namely: (1) H^+ mobility concerns the properties of fuel cells (hydrogen technology). (2) Li^+ mobility properties are essential for "electro-mobility" (e.g. batteries, cars).

Concluding, the present author believes that the theoretical formalism of WV, and TSVF not only sheds new light on interpretational issues concerning fundamental quantum theory (like e.g. the time-inversion invariance of the basic physical laws, the meaning of quantum entanglement and correlations, etc.) but it also offers a fascinating new guide for our intuition to predict new effects, and further helps to design and perform new experiments and reveal novel quantum phenomena.

Acknowledgments
I wish to thank E. Irran and Th.-Ch. Rdel (TU Berlin) for fruitful collaboration and assistance by the XRD measurements; and Ph. Stammer (TU Berlin) for helpful discussions on the theory of WV and TSVF. Last but not least, I thank the organizers and the participants of the SiS Conference Series during the past 10 years for stimulating and inspiring talks and discussions.

[1] Aharonov Y and Rohrlich D 2005 *Quantum Paradoxes: Quantum Theory for the Perplexed* (Weinheim: Wiley-VCH)
[2] Aharonov Y, Bergmann P G and Lebowitz J L 1964 *Phys. Rev.* **134**, B1410
[3] Aharonov Y, Albert D Z and Vaidman L 1988 *Phys. Rev. Lett.* **60** 1351
[4] Aharonov Y and Vaidman L 1990 *Phys. Rev. A* **41** 11
[5] Tamir B and Cohen E 2013 *Quanta* **2** 7
[6] Aharonov Y, Cohen E and Elitzur A C 2014 *Phys. Rev. A* **89** 052105
[7] Aharonov Y, Cohen E, Waegell M and Elitzur A C 2018 *Entropy* **20** 854
[8] Shikano Y 2012 *Theory of Weak Value" and Quantum Mechanical Measurements*, in: Measurements in Quantum Mechanics, Reza Pahlavani M (Ed.), pp. 75-100; (Shanghai and Rijeka: InTech)
[9] N. W. M. Ritchie, J. G. Story, and Randall G. Hulet 1991 *Phys. Rev. Lett.* **66** 1107
[10] Lundeen J S, Sutherland B, Patel A, Stewart C and Bamber C 2011 *Direct measurement of the quantum wavefunction. Nature* **474** 188-191
[11] Dressel J, Malik M, Miatto F M, Jordan A N and Boyd R W 2014 *Rev. Mod. Phys.* **86** 307
[12] Feynman; R. P.; Leighton, R. B.; Sands, M. *The Feynman Lectures on Physics, Vol. III, Quantum Mechanics*; Addison-Wesley Publ.: Reading, USA, 1965. [Also available at: http://www.feynmanlectures.caltech.edu/]
[13] Jozsa R 2007 *Phys. Rev. A* **76** 044103
[14] Pati, A. K.; Wu, J. Conditions for anomalous weak value. *ArXiv* 2014; arXiv:1410.5221v1 [quant-ph].
[15] Chatzidimitriou-Dreismann C A 2016 *Quanta* **5** 61-84
[16] Chatzidimitriou-Dreismann C A 2018 *J. Phys.: Conf. Ser.* **1071** 012007
[17] Chatzidimitriou-Dreismann C A 2019 *Universe* **5** 58; https://doi.org/10.3390/universe5020058
[18] Elitzur A.C and Vaidman L 1993 *Found. Phys.* **23** 987-997
[19] Arute F, et al. 2019 *Quantum supremacy using a programmable superconducting processor. Nature* **574** 505-510
[20] Wang H, et al. 2019 *Boson sampling with 20 input photons and a 60-Mode interferometer in a* 10^{14}*-dimensional Hilbert space. Phys. Rev. Lett.* **123** 250503
[21] Aharonov Y, Botero A, Nussinov S, Popescu S, Tollaksen J and Vaidman L 2013 *New J. Phys.* **15** 093006
[22] Scully M O and Zubairy M S 1997 *Quantum Optics* (Cambridge: Cambridge University Press)
[23] von Neumann J 1955 *Mathematical Foundations of Quantum Mechanics* (Princeton: Princeton University Press)
[24] Squires G L 2012 *Introduction to the Theory of Thermal Neutron Scattering* (Cambridge: Cambridge University Press)
[25] Watson G I 1996 *J. Phys.: Condens. Matter* **8** 5955
[26] van Hove L 1954 *Phys. Rev.* **95** 249
[27] https://neutrons.ornl.gov/ARCS
[28] Diallo S O, Azuah R T, Abernathy D L, Rota R, Boronat J and Glyde H R 2012 *Phys. Rev. B* **85** 140505
[29] Aharonov Y, Cohen E and Ben-Moshe S 2014 *EPJ Web of Conferences* **70**, 00053
[30] Olsen R J, Beckner M, Stone M B, Pfeifer P, Wexler C and Taub H 2013 *Carbon* **58** 46
[31] Mitchell P C H, Parker S F, Ramirez-Cuesta A J and Tomkinson J 2005 *Vibrational Spectroscopy with Neutrons.* (New Jersey: World Scientific)
[32] Georgiev P A, Ross D K, De Monte A, Montaretto-Marullo U, Edwards R A H, Ramirez-Cuesta A J, Adams M A and Colognesi D 2005 *Carbon* **43** 895
[33] http://www.isis.stfc.ac.uk/instruments/TOSCA/
[34] Dirac P A M 1957 *The Principles of Quantum Mechanics* 4th ed. (Oxford: Clarendon Press)
[35] Chantler C T, Rae N A and Tran C Q 2007 *J. Appl. Cryst* **40** 232-240
[36] Vaidman L 2014 *Comment on "How the result of a single coin toss can turn out to be 100 heads"* ArXiv:1409.5386 [quant-ph]
[37] Xu M, Ye S, Powers A, Lawler R, Turro N J and Bačić Z 2013 *J. Chem. Phys.* **139** 064309
[38] Poirier B 2015 *J. Chem. Phys.* **143** 101104
[39] Ferrie C and Combes J 2014 *Phys. Rev. Lett.* **113** 120404
[40] Romito A, Jordan A N, Aharonov Y and Gefen Y 2016 *Quantum Studies: Mathematics and Foundations* **3** 1
[41] Horodecki R, Horodecki P, Horodecki M and Horodecki K 2009 *Rev. Mod. Phys.* **81** 865

[42] Nielsen M A and Chuang I L 2010 *Quantum Computation and Quantum Information* (Cambridge: Cambridge University Press)
[43] Arora S and Barak B 2009 *Computational Complexity – A Modern Approach* (Cambridge: Cambridge University Press)
[44] Fortnow L 2009 *Communications of the ACM* **52** 78
[45] Papadimitriou C H 1995 *Computational Complexity* (Reading: Addison-Wesley)